iScience

CellPress
OPEN ACCESS

Article

AIM2 promotes T_H17 cells differentiation by regulating RORγt transcription activity

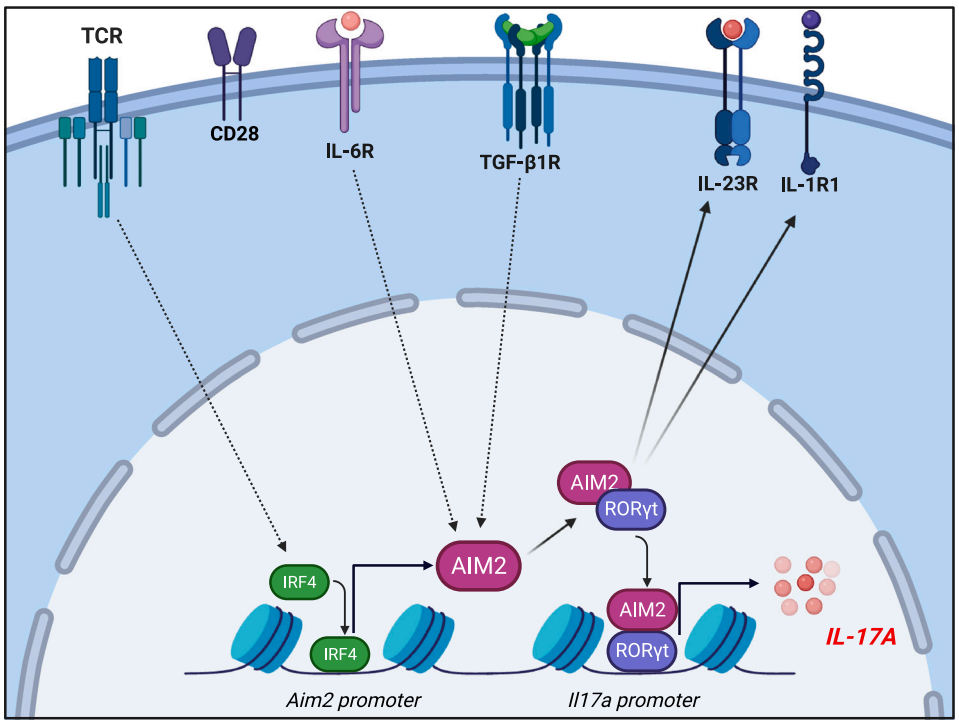

Jefferson Antônio Leite, Luísa Menezes, Eloisa Martins, ..., Ari Waisman, Daniela Carlos, Niels Olsen Saraiva Câmara

jeffersonleite@usp.br (J.A.L.)
waisman@uni-mainz.de (A.W.)
danicar@usp.br (D.C.)
niels@icb.usp.br (N.O.S.C.)

Highlights

AIM2 is crucial for the optimal differentiation of Th17 cells and IL-17A production

The absence of AIM2 in $CD4^+$ T cells was associated with a failure to induce colitis in mice

IRF4 regulates AIM2 expression during Th17 cell differentiation

AIM2's nuclear interaction with RORγt boosts Th17 differentiation and IL-17A production

Leite et al., iScience *26*, 108134
November 17, 2023
https://doi.org/10.1016/j.isci.2023.108134

iScience

CellPress
OPEN ACCESS

Article

AIM2 promotes T_H17 cells differentiation by regulating RORγt transcription activity

Jefferson Antônio Leite,[1,4,7,*] Luísa Menezes,[4] Eloisa Martins,[4,5] Tamara Silva Rodrigues,[1,3] Lucas Tavares,[3] Anna Ebering,[7] Carsten Schelmbauer,[7] Guilherme C. Martelossi Cebinelli,[1,2] Valeriya Zinina,[7] Artemiy Golden,[7] Natalia Soshnikova,[7] Dario S. Zamboni,[3] Fernando Q. Cunha,[2] Magdalena Huber,[8] João Santana Silva,[1,6] Ari Waisman,[7,*] Daniela Carlos,[1,*] and Niels Olsen Saraiva Câmara[1,4,5,9,*]

SUMMARY

AIM2 is an interferon-inducible HIN-200 protein family member and is well-documented for its roles in innate immune responses as a DNA sensor. Recent studies have highlighted AIM2's function on regulatory T cells (Treg) and follicular T cells (Tfh). However, its involvement in Th17 cell differentiation remains unclear. This study reveals that AIM2 promotes Th17 cell differentiation. AIM2 deficiency decreases IL-17A production and downregulates key Th17 associated proteins (RORγt, IL-1R1, IL-23R). AIM2 is located in the nucleus of Th17 cells, where it interacts with RORγt, enhancing its binding to the Il17a promoter. The absence of AIM2 hinders naive CD4 T cells from differentiating into functional Th17 cells and from inducing colitis in Rag1$^{-/-}$ mice. This study uncovers AIM2's role as a regulator of Th17 cell transcriptional programming, highlighting its potential as a therapeutic target for Th17 cell-mediated inflammatory diseases.

INTRODUCTION

The *absent in melanoma* 2 (AIM2) is a protein belonging to the interferon-inducible HIN-200 protein family,[1] first described as a tumor growth suppressor gene.[2] Expression of AIM2 is induced after exposure to IFN-γ,[3] but unlike other members of the interferon-inducible family, AIM2 has a cytoplasmic localization.[4] AIM2 was shown to be involved in innate immunity by acting as a double-stranded DNA (dsDNA) sensor.[5–7] In macrophages, AIM2 is expressed in the cytosol where it can directly bind to dsDNA from pathogens or self-DNA from death cells. The binding of DNA to AIM2 initiate the assembly of the AIM2 inflammasome. The PYD domain of AIM2 binds directly to the PYD domain of ASC, which then interacts with CARD domain of caspase-1 leading to the recruitment of caspase-1, and subsequent processing of pro-IL1β, pro-IL 18 and gasdermin-D (GSDMD).[5–7] Similar functions of AIM2 were reported in dendritic cells in models of bacterial and virus infections.[8,9]

Previously, Komori and colleagues demonstrated that AIM2 is highly expressed in activated memory CD4 T cells;[10] however, how its expression regulates the function of these cells remains unknown. Like other helper T cells, Treg cells also express AIM2.[11] Indeed, the deletion of AIM2 specifically in Treg cells leads to a reduced expression of FoxP3 and is associated with the reduced suppressive function of these cells.[12] In addition, we recently demonstrated in a Type 1 diabetes (T1D) model that AIM2-deficient mice have a reduction in IL-17A production by CD4 T cells. The production of IL-17A by AIM2-deficient CD4 T cells was significantly reduced in pancreatic lymph nodes (PLNs) and gut mucosal of Aim2$^{-/-}$ mice, leading to the hypothesis that an intrinsic expression of AIM2 in CD4 T cells could promote Th17 differentiation.[13]

In this study, we demonstrated that AIM2 has a T cell-intrinsic and inflammasome-independent role in the differentiation and function of Th17 cells. AIM2 is highly expressed throughout Th17 differentiation, and its promoter is occupied by Th17 cell-related transcription factors such as IRF4, FOSL2, MAF, p300, BATF, CTCF, and STAT3. AIM2 is required for optimal Th17 cell development and IL-17A production, as well as for the expression of the transcription factor RORγt. Mechanistically, AIM2 translocates to the nucleus and physically interacts with RORγt, enhancing its binding activity in the Il17a promoter region to promote Th17 cell development. Thus, AIM2 is relevant for Th17 cell differentiation *in vivo* by enhancing T cell-mediated intestinal inflammation.

[1]Department of Biochemistry and Immunology, Ribeirão Preto School of Medicine, University of São Paulo, Ribeirão Preto, São Paulo, Brazil
[2]Department of Pharmacology, Ribeirão Preto School of Medicine, University of São Paulo, Ribeirão Preto, São Paulo, Brazil
[3]Department of Cellular and Molecular Biology and Pathogenic Bioagents, Ribeirão Preto School of Medicine, University of São Paulo, Ribeirão Preto, São Paulo, Brazil
[4]Department of Immunology, Institute of Biomedical Sciences, University of Sao Paulo, São Paulo, Brazil
[5]Division of Nephrology, School of Medicine, Federal University of São Paulo, São Paulo, Brazil
[6]Fiocruz-Bi-Institutional Translational Medicine Project, University of São Paulo, Ribeirão Preto, São Paulo, Brazil
[7]Institute for Molecular Medicine, University Medical Center of the Johannes Gutenberg-University Mainz, Mainz, Germany
[8]Institute of Systems Immunology, Center for Tumor and Immunology, University of Marburg, Marburg, Germany
[9]Lead contact
*Correspondence: jeffersonleite@usp.br (J.A.L.), waisman@uni-mainz.de (A.W.), danicar@usp.br (D.C.), niels@icb.usp.br (N.O.S.C.)
https://doi.org/10.1016/j.isci.2023.108134

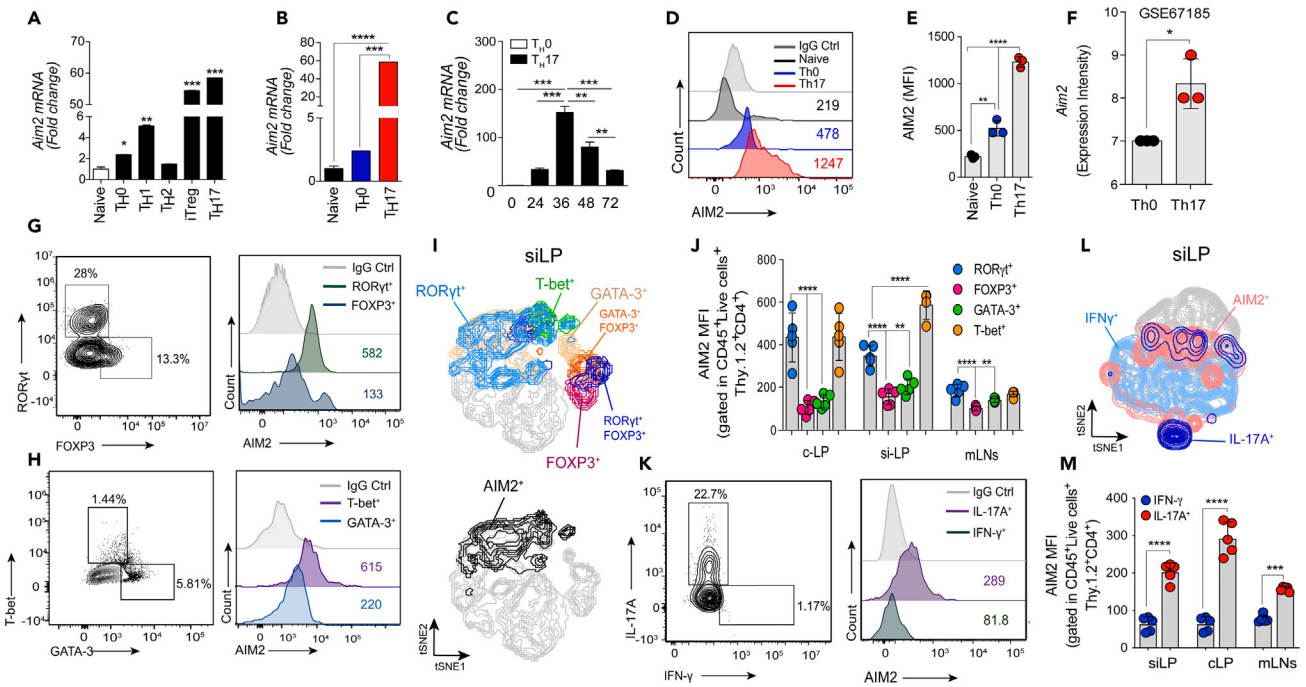

Figure 1. AIM2 is expressed in Th17 cells

(A) AIM2 mRNA expression in naive, activated CD4 T cells (Th0), Th1, Th2, iTreg and Th17 at 96 h of culture. Fold change relative to naive cells (n = 3).

(B) AIM2 mRNA expression in naive, activated CD4 T cells (Th0) and Th17 at 72 h of culture. Fold change relative to naive cells (n = 3).

(C) Kinetics analysis of AIM2 mRNA expression during Th17 cells differentiation. Fold change relative to Th0 (n = 3).

(D) Histogram of flow cytometric analysis of AIM2 expression in naive, activated CD4 T cells (Th0) and Th17 cells at 96 h of culture. Gate strategy (Live cells + CD4 + IL-17A + AIM2 +).

(E) Mean of the fluorescence intensity of AIM2 in naive, activated CD4 T cells (Th0) and Th17 cells at 96 h of culture. Gate strategy (Live cells + CD4 + IL-17A + AIM2+) (n = 3).

(F) Microarray expression intensity of AIM2 in human *in vitro* differentiated activated CD4 T cells (Th0) and Th17 cells. Data obtained from a public available dataset from NCBI dataset (GSE67185) and analyzed with GEO2R (n = 3).

(G–I) Representative flow cytometric analysis of AIM2 expression in RORγt+, FOXP3+, T-bet+. GATA = 3+ CD4 T cells in colonic lamina propria (c-LP) (Gate in CD45+Live cells + Thy.1.2 + $CD4^+$) (n = 5).

(J) Mean of fluorescence intensity (MFI) of AIM2 expression in RORγt+, FOXP3+, T-bet+, GATA-3+ CD4 T cells in colonic lamina propria (c-LP), small intestine lamina propria (si-LP) and mesenteric lymph nodes (mLNs) of an 8-week-old naive mouse (n = 5).

(K and L) Representative flow cytometric analysis of AIM2 expression in IL-17A+ and IFNγ+ CD4 T cells in colonic lamina propria (c-LP) (Gate in CD45+Live cells + Thy.1.2 + $CD4^+$) (n = 5).

(M) Mean of fluorescence intensity (MFI) of AIM2 expression in IL-17A+ and IFNγ+ CD4 T cells in c-LP, si-LP and mLNs of an 8-week-old naive mouse (n = 5). Data are representative of at least two independent experiments and are shown as mean ± SEM. *p < 0.05 determined by one-way ANOVA followed by Tukey's post hoc test.

RESULTS

The expression of AIM2 is increased during Th17 differentiation

In order to study the role of AIM2 in T cells, we first examined the expression of AIM2 in T helper (Th) subtypes. To do this, we cultured naive $CD4^+CD62L^{high}$ T cells under Th1, Th2, Th17 and induced Treg (iTreg) cell-polarizing conditions. As controls, we used naive $CD4^+CD62L^{high}$ T cells and activated $CD4^+CD62L^{high}$ T cells with plate bounded anti-CD3ε/CD28 without the addition of differentiation cytokines (hereafter, Th0). We observe that *Aim2* mRNA is upregulated at different levels in all Th subtypes, except Th2 (Figure 1A). In addition, *Aim2* mRNA expression was significantly higher in Th17 cells (Figures 1A and 1B), peaking at 36h of culture (Figure 1C). In accordance, we found increased protein levels of AIM2 in Th17 cells when compared to naive $CD4^+CD62L^{high}$ T cells and Th0 (Figures 1D and 1E). Next, we sought to we determine if AIM2 is expressed also in human Th17 cells. To this end, we performed *in silico* analysis of the publicly available dataset (GSE67185) using NCBI datasets and GEO2R. Importantly, we found that *Aim2* is significantly upregulated in Th17 cells when compared to Th0 (Figure 1F).

Next, we determined the expression of AIM2 *in vivo* in cells isolated from the gut mucosa, a place enriched with Th17 cells under homeostatic conditions (*21*). We evaluated its expression in harvested cells from mesenteric lymph nodes (mLNs), small intestine lamina propria (si-LP) and colonic lamina propria (c-LP) and in different populations of Th subtypes according to their transcription factors and cytokines.

We detected an increased expression of AIM2 in RORγt and T-bet expressing $CD4^+$ T cells at the c-LP and si-LP when compared to GATA-3^+ and $FoxP3^+$ $CD4^+$ T cells (Figures 1G–1J). In the mLNs, AIM2 was significantly expressed in RORγt^+ $CD4^+$ T cells (Figures 1G and 1J). IL-17A-producing $CD4^+$ T cells expressed high levels of AIM2 in the si-LP, c-LP and mLNs when compared to IFN-γ-producing $CD4^+$ T cells (Figures 1K–1M).

Th17 cells requires AIM2 for an optimal differentiation

To determine whether AIM2 is involved in the differentiation of Th17 cells we sorted $CD4^+CD62L^{high}$ T cells from LNs and spleen of WT and *Aim2*$^{-/-}$ mice and cultured these cells under Th17 cells polarizing conditions for five days. Interestingly, the frequency of IL-17A producing cells generated from *Aim2*$^{-/-}$ mice was lower than WT (Figures 2A and 2B), and was associated with decreased IL-17A levels secreted in the culture supernatant (Figure 2C) *and Il17a* mRNA expression (Figure 2D). However, no differences were found in the mRNA levels of *il22* (Figure 2E) and the deficiency of AIM2 in CD4 T cells did not alter the proliferation and the survival of Th17 cells (Figures S1A–S1D). Consistent with the reduced Th17 cell differentiation, the expression of the Th17 cells-related genes, *Rorc, Rorα, Stat3, Il23r, Il1r1* and *Il17a,* were reduced while both mRNA and protein expression of *Foxp3* was increased in *Aim2*$^{-/-}$ Th17 cells (Figures 2F, S2E, and S2F). In agreement, we found that also the protein levels of RORγt, as well as the receptors IL-1 and IL-23 were reduced in the Th17 that developed in the absence of *Aim2* (Figures 2F–2L).

IL-6 and IL-23 induced Th17 cell differentiation via STAT3 activation (*25, 26*). Since we observed that *Stat3* mRNA was downregulated in *Aim2*-deficient Th17 cells, we next evaluated if *Aim2* deficiency affected STAT3 phosphorylation, but found it to be unaltered (Figures S2A and S2B). Similar findings were obtained when we stimulated $CD4^+CD62L^{high}$ T cells with IL-6 (Figures S2C and S2D). Taken together, these results demonstrated that AIM2 promotes Th17 cells independent of STAT3 signaling pathway.

Next, we investigated if AIM2 was important for IL-17A production in CD4 T cells *in vivo*. To this end, we isolated mLNs and spleen cells from WT and *Aim2*$^{-/-}$ mice and stimulated the cells with plate-bound α-CD3ε and α-CD28 for 24h and the production of IL-17A and IFN-γ were measured. Interestingly, we observed that mLNs and SP CD4 T cells produced significantly less IL-17A in the absence of AIM2 when compared to WT CD4 T cells, as well as secreted less IL-17A (Figures S3A and S2B). The amount of IFN-γ was similar between both WT and *Aim2*$^{-/-}$ CD4 T cells (Figures 3A, 3D, and 3E).

Finally, we sorted effector/memory CD4 T cells ($CD44^{high}CD25^-CD4^+$) from pooled splenocytes and lymph nodes of WT and *Aim2*$^{-/-}$ mice, stimulated them with plate-bound α-CD3ε and α-CD28 for 24h and evaluated the production of IL-17A. In the absence of AIM2, effector/memory CD4 T cells produced less IL-17A and significantly expressed less *Il17a* mRNA when compared WT CD4 T cells (Figures 2M–2O). In addition, the production of IL-17A by leukocytes isolates from spleen, si-LP/c-LP from Aim2$^{-/-}$ animals secreted less IL-17A after 24h of stimulation with plate-bound α-CD3ε and α-CD28 (Figures 2P and 2Q). Collectively, these results demonstrated that AIM2 expression in CD4 T cells is required for Th17 cells development and IL-17A production.

AIM2-deficient $CD4^+$ T cells fail to differentiate into IL-17A$^+$/IFN-γ$^+$ producing cells and to induce T cell-induced colitis in Rag1$^{-/-}$ mice

In order to understand if the absence of AIM2 in $CD4^+$ T cells alters their function and differentiation *in vivo*, we sorted $CD4^+CD45RB^{high}$ naive T cells from WT and *Aim2*$^{-/-}$ mice and transferred into Rag1$^{-/-}$ mice and monitored for the development of colitis. In contrast to Rag1$^{-/-}$ mice receiving WT CD4 T cells, mice that received *Aim2*$^{-/-}$ CD4 T cells did not lose weight or shorten colon length and had less colon inflammation (Figures 3A–3E). In agreement, endoscopy analysis showed less signs of granularity, fibrin and diarrheic stool in Rag1$^{-/-}$ mice which were transferred with *Aim2*$^{-/-}$ CD4 T cells, which indicates that the transference of AIM2-deficient CD4 T cells were not colitogenic (Figure 3F).

Next, we evaluated the cytokine production by WT and *Aim2*$^{-/-}$ CD4 T cells in mLNs and c-LP of Rag1$^{-/-}$ mice 4 weeks after T cell transfer. The frequency and numbers of TCR-β$^+$CD4$^+$IL17A$^+$ and TCR-β$^+$CD4$^+$IL17A$^+$ IFN-γ$^+$ producing cells were significantly reduced in mice transferred with AIM2-deficient CD4 T cells when compared to Rag1$^{-/-}$ transferred with WT CD4 T cells (Figures 3G–3I, 3L, and 3M) whereas the frequency of TCR-β$^+$CD4$^+$IFN-γ$^+$ were decreased in mLNs in the absence of AIM2, however, there is no differences in TCR-β$^+$CD4$^+$IFN-γ$^+$ in mice transferred with AIM2-deficient CD4 T cells when compared to Rag1$^{-/-}$ transferred with WT CD4 T cells (Figures 3J and 3K). In addition, the expression of TCR-β$^+$CD4$^+$ RORγt^+ and TCR-β$^+$CD4$^+$FOXP3$^+$ cells were reduced in mice transferred with AIM2-deficient CD4 T cells when compared to Rag1$^{-/-}$ transferred with WT CD4 T cells (Figures S4A–S4G).

Taken together, these results demonstrated that the absence of AIM2 in $CD4^+$ T cells fails to induce colitis in Rag1$^{-/-}$ and this was associated with lower frequency of Th17 cells, which indicated that AIM2 expression in CD4 T cells promotes Th17 cells differentiation *in vivo*.

AIM2 function in Th17 cells is independent of dsDNA sensing and inflammasome activation

Next, we sought a possible mechanism by which AIM2 drives Th17 cell differentiation. The classical function of AIM2 is related to the dsDNA recognition and activation of inflammasome. Previous studies have already reported that inflammasome can be activated and may enhance Th17 cell differentiation (*27*). Thus, we hypothesized that the recognition of dsDNA by AIM2 could promote Th17 cells differentiation. To evaluate if AIM2 activates the inflammasome in Th17 cells, we sorted naive $CD4^+CD62L^{high}CD44^{low}$ T cells from WT and *Aim2*$^{-/-}$ animals, and differentiated the cells under Th17 cells polarizing condition, in the presence or absence of transfected poly dA:dT. We found that poly dA:dT was not able to induce caspase-1 activation and IL-1β production (Figures 4A–4D). In addition, Th17 cells produced similar levels of IL-17A when the cells were differentiated in the presence of poly dA:dT (Figure 4E). Moreover, we detected similar levels of cleaved caspase-1 in the culture supernatant when WT and *Aim2*$^{-/-}$ Th17 cells were stimulated with poly dA:dT (Figures 4F–4H).

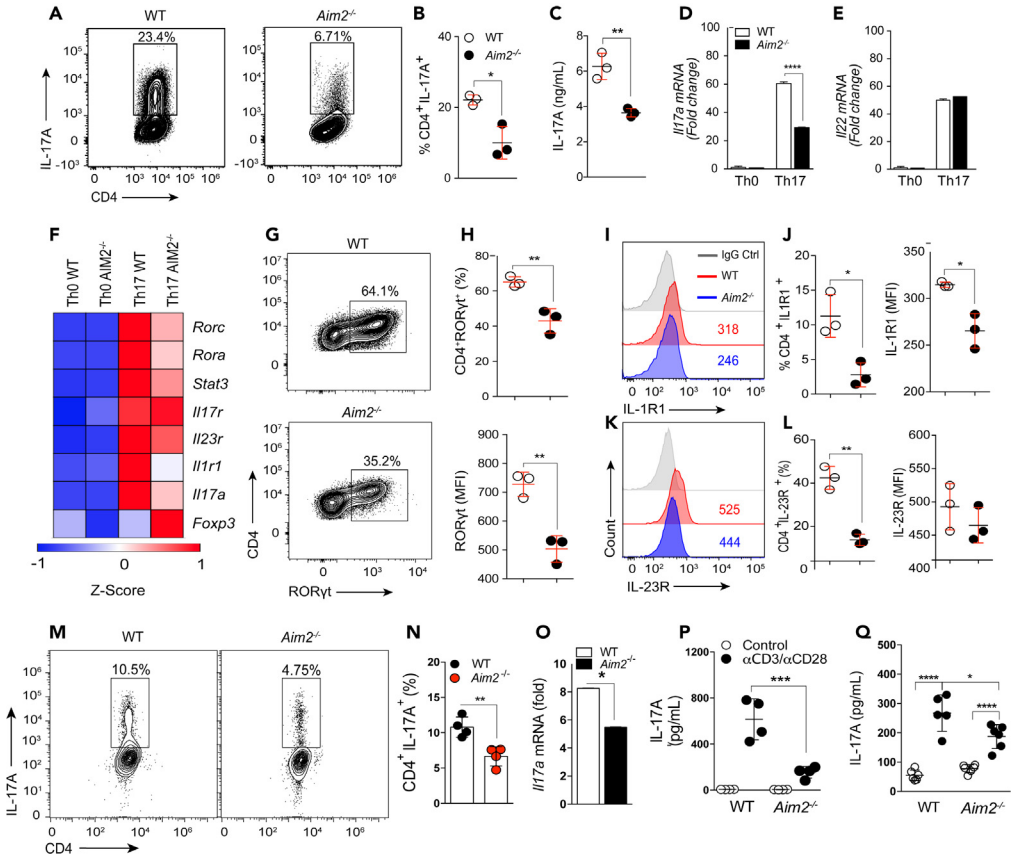

Figure 2. AIM2 is a positive regulator of Th17 cell differentiation

(A) Representative flow cytometric analysis of IL-17A expression by WT and Aim2−/− Th17 cells at 96 h of culture. Gate strategy (Live cells+CD4+IL-17A+) (n = 3).
(B) Frequency of WT and Aim2−/− CD4+IL-17A + at 96 h of culture accessed by flow cytometric analysis (n = 3).
(C) IL-17A protein levels in the supernatant of WT and Aim2−/− Th17 cells at 96 h of culture accessed by enzyme-linked immunosorbent assay (ELISA) (n = 3).
(D and E) Il17a and Il-22 mRNA expression in WT and Aim2−/− Th0 and Th17 at 96 h of culture. Fold change is relative to WT Th0 (n = 3).
(F) Heatmap representing the mRNA expression of Rorc, Rora, Stat3, Il17r, Il23r, Il1r1, Il17a and Foxp3 in WT and Aim2−/− Th0 and Th17 at 96 h of culture. Fold change is relative to WT Th0 (n = 3).
(G) Representative flow cytometric analysis of RORγt expression by WT and Aim2−/− Th17 cells at 96 h of culture. Gate strategy (Live cells+CD4+RORγt+) (n = 3).
(H) Frequency and mean of fluorescence intensity (MFI) of WT and Aim2−/− CD4+RORγt+ at 96 h of culture accessed by flow cytometric analysis (n = 3).
(I) Representative flow cytometric analysis of IL-1R1 expression by WT and Aim2−/− Th17 cells at 96 h of culture. Gate strategy (Live cells+CD4+IL-1R1+) (n = 3).
(J) Frequency and mean of fluorescence intensity (MFI) of IL-1R1 expression in WT and Aim2−/− Th17 cells at 96 h of culture (n = 3).
(K) Representative flow cytometric analysis of IL-23R expression by WT and Aim2−/− Th17 cells at 96 h of culture. Gate strategy (Live cells+CD4+IL-23R+) (n = 3).
(L) Frequency and mean of fluorescence intensity (MFI) of IL-23R expression in WT and Aim2−/− Th17 cells at 96 h of culture (n = 3).
(M) Counter plot representing the frequency of CD4+IL-17A + cells (gate inside viable cells) after the sorting of $CD4^+CD25^-CD44high$ cells from spleen and lymph node samples from WT and AIM2−/− mice. Cells were stimulated with anti-CD3/CD28 for 24 h.
(N) Frequency of CD4+IL-17A + cells ($CD4^+CD25^-CD44high$) from spleen and lymph node samples from WT and AIM2−/− mice after 24 h of stimulation with anti-CD3/28.
(O) Il17a mRNA levels in $CD4^+CD25^-CD44high$ WT and AIM2−/− cells after 24 h of stimulation with anti-CD3/CD28.
(P and Q) Protein levels of IL-17A in the supernatant of cultures of leukocytes isolated from the spleen and intestinal lamina propria (small intestine and colon) from WT and AIM2−/− mice and stimulated for 24 h with anti-CD3/CD28. Data are representative of at least two independent experiments and are shown as mean ± SEM. *p < 0.05 determined by one-way ANOVA followed by Tukey's post hoc test or T-test *p < 0.05.

Immunofluorescence analysis demonstrated a nuclear localization of AIM2 in Th17 cells without poly dA:dT stimulation, but when Th17 cells were stimulated, an AIM2 puncta was detected in the cytosol (Figures 4I–4K). Taken together, these results suggest that AIM2 promotes the differentiation of Th17 cells independent of its DNA sensor function and inflammasome activation.

The expression of AIM2 in Th17 cells is regulated by IRF4

Next, we aimed to evaluate the factors involved in the regulation of AIM2 expression during Th17 cell differentiation. First, we assessed if the cytokines TGF-β and IL-6, involved in the differentiation of Th17 cells, could induce the expression of AIM2 in activated CD4 T cells.

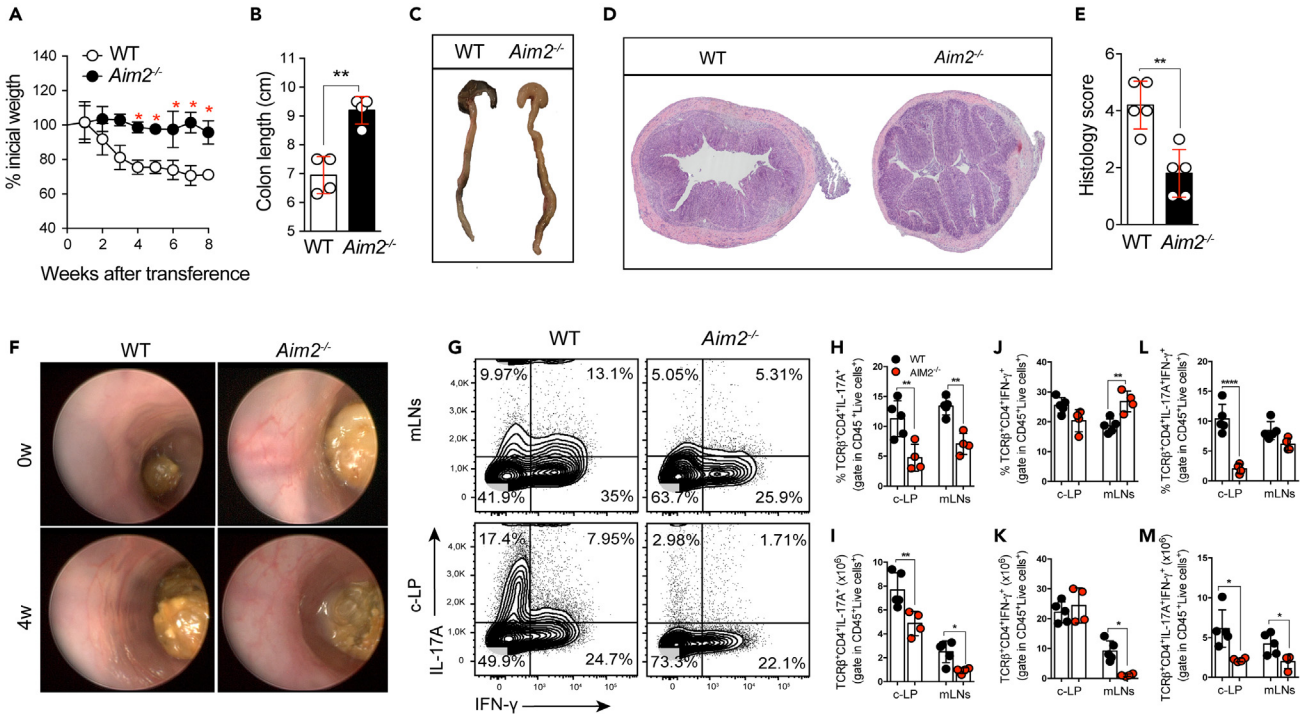

Figure 3. AIM2 promotes T cell transfer colitis in Rag1−/− mice by enhancing Th17 cell differentiation

(A) Frequency of initial weight of Rag1−/− mice 0, 2, 4, 6, and 8 weeks after transfer of $CD4^+CD45RBhigh$ T cells isolated from WT and Aim2−/− mice (n = 4).

(B and C) Colon length of Rag1−/− mice 8 weeks after transfer of $CD4^+CD45RBhigh$ T cells isolated from WT and Aim2−/− mice (n = 4).

(D and E) Histology and histology score of the colon of Rag1−/− mice 4 weeks after transfer of $CD4^+CD45RBhigh$ T cells isolated from WT and Aim2−/− mice (n = 4–5).

(F) Colon endoscopy of Rag1−/− mice 0 and 4 weeks after transfer of $CD4^+CD45RBhigh$ T cells isolated from WT and Aim2−/− mice (n = 4–5).

(G) Representative flow cytometric analysis of the frequency of TCR-β+CD4+IL-17A+, TCR-β+CD4+IFN-γ+, and TCR-β+CD4+IL-17A+IFN-γ+ cells (gated within $CD45^+$ cells and viable cells) in colonic lamina propria (c-LP), mesenteric lymph nodes (mLNs) from Rag1−/− mice 4 weeks after transfer of $CD4^+CD45RBhigh$ T cells isolated from WT and Aim2−/− mice (n = 4–5).

(H and I) Frequency and absolute number of TCR-β+CD4+IL-17A+, (J and K) TCR-β+CD4+IFN-γ+, and (L and M) TCR-β+CD4+IL-17A+IFN-γ+ cells (gated within $CD45^+$ cells and viable cells) in colonic lamina propria (c-LP), mesenteric lymph nodes (mLNs) from Rag1−/− mice 4 weeks after transfer of $CD4^+CD45RBhigh$ T cells isolated from WT and Aim2−/− mice (n = 4–5). Data are representative of at least two independent experiments and are shown as mean ± SEM. *p < 0.05 determined by one-way ANOVA followed by Tukey's post hoc test or T-test *p < 0.05.

Interestingly, the stimulation of activated CD4 T cells with TGFβ induced a significant expression of AIM2, which was even more pronounced by the addition of IL-6, but not by this cytokine alone (Figure 5A). The stimulation of Th17 cells with different amounts of TGFβ and IL-6, significantly increased *Aim2* mRNA expression, along with increased expression of *Rorc*, *Stat3* and *Il17a* (Figures 5B–5D).

To better understand the mechanisms that drive the expression of AIM2 in Th17 cells we took advantage of the Cistrome Project[14] and used their data browser tool to analyze public available ATAC-seq and ChIP-seq data to understand the transcription regulation of AIM2 expression in Th17 cells. First, we used the Cistrome DB toolkit, to predict the transcription factors that regulate AIM2 expression in Th17 cells. Interestingly, we found an increased regulatory potential score of IRF4, CTCF and JMJD6 at the *Aim2* locus in Th17 cells which suggests that these factors could possibly regulate positively or negatively *Aim2* expression in Th17 cells (Figure 5E). In agreement, we found several ATAC-seq peaks at *Aim2* locus in Th17 cells when compared to Th0 (Figure 5F). These ATAC-seq peaks were associated with H3K4me3-binding peaks at the *Aim2* promoter region in Th17 cells when compared to Th0 (Figure 5F). We also found that the *Aim2* promoter region can be occupied by several transcription factors involved in Th17 cells differentiation, namely IRF4, FOSL2, MAF, p300, BATF, CTCF and STAT3 (Figures 5F and S5A). Previous studies demonstrated that IRF4 is an important regulator of Th17 cells differentiation.[15–17] Thus, we next evaluated if the deficiency of IRF4 affects the expression of AIM2 in Th17 cells. To this end, we inhibited IRF4 expression using short hairpin RNA (IRF4 shRNA) to investigate *Aim2* expression. Indeed, the expression of *Aim2* mRNA was also decreased in IRF4-shRNA treated Th17 cells (Figures 5G and 5H). Additionally, the expression of *Aim2* mRNA in IRF4-deficient Th17 cells was downregulated when compared to WT Th17 cells (Figures 5I and 5J). In addition, the knockdown of IRF4 expression using short hairpin RNA (IRF4 shRNA) significantly reduces the protein expression of IRF4 as well as AIM2 in Th17 cells (Figures 5K–5M).

Taken together, these results demonstrated that AIM2 is expressed in Th17 cells, and its expression is regulated by IRF4.

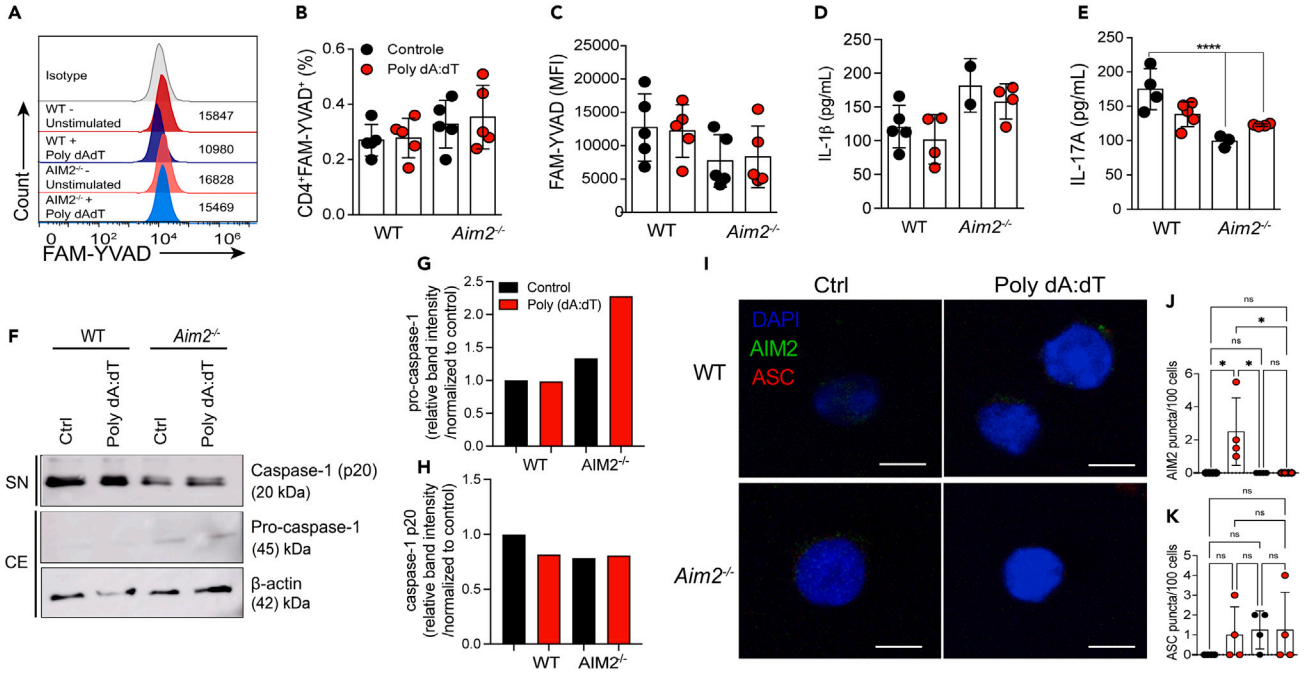

Figure 4. Activation of AIM2 by dsDNA in Th17 cells

(A) Histogram representing the frequency of Th17 lymphocytes FAM-YVAD+ after stimulation with Poly dA:dT (n = 5).

(B and C) Frequency and mean of fluorescence intensity CD4+IL-17A+ FAM-YVAD+ WT and AIM2−/− cells after stimulation with Poly dA:dT (n = 5).

(C) IL-1β levels detected in the supernatant of cultures Th17 cells stimulated with Poly dA:dT or culture medium alone (n = 5).

(E) IL-17A levels in the supernatant of cultured Th17 cells stimulated with Poly dA:dT or culture medium alone (n = 5).

(F) Immunoblot analysis of caspase-1 in supernatant (SN) and cellular extracts (CE) of Th17 cells stimulated with Poly dA:dT or culture medium alone (n = 5).

(G and H) Densitometric quantification of pro-capase-1 and activate caspase 1.

(I) Confocal immunofluorescence microscopy of AIM2, ASC and DAPI in WT and Aim2KO Th17 cells stimulated with Poly dA:dT or culture medium alone (n = 4).

(J and K) AIM2 or ASC puncta per 100 cells in WT and Aim2KO Th17 cells stimulated with Poly dA:dT or culture medium alone (n = 4). Results are considered statistically significant when $p < 0.05$, and asterisks (*) represent the level of significance according to the p value. N = 3–5. Significant differences between groups were determined by one-way ANOVA.

AIM2 interacts with RORγt and enhances its transcription activity

AIM2 plays non-canonical functions in B and T cells by translocating into the nucleus and interacting with transcriptions factors such as BCL-6 and Blimp-1 in B cells[18] or c-MAF in follicular T helper cells (Tfh).[11] Because our results demonstrated that AIM2 promotes Th17 cells differentiation independent of its DNA sensor function and inflammasome activation, a role that AIM2 exerts in the cytosol, we next evaluated in which cell compartment AIM2 is expressed in Th17 cells. To this end, we performed *in vitro* differentiation of Th17 and activated CD4 T cells (Th0) and analyzed for AIM2 in cytosolic and nuclear fractions. We observe an increased expression of AIM2 in the nuclear fractions of Th17 cells when compared to the cytosolic fractions and when compared with the nuclear fractions of Th0 cells (Figures 6A and 6B). Confocal immunofluorescence microscopy showed that Th17 cells stain punctate for AIM2, whereas Th0 cells stain for AIM2 in the cytoplasm. (Figure 6C).

As we found that RORγt expression was compromised in *Aim2*-deficient Th17 cells, we investigated whether AIM2 and RORγt can interact during the development of Th17 cells. We performed *in vitro* Th17 cells differentiation and harvested the cells at 36h of culture, the time we found that *Aim2* expression was increased (Figure 1E) to perform co-immunoprecipitation analysis. Indeed, we found that AIM2 co-immunoprecipitated with RORγt (Figure 6D). In line with this, confocal microscopy analysis demonstrated a co-localization between AIM2 and RORγt in the nucleus of Th17 cells (Figure 6E). To further confirm that the interaction between AIM2 and RORγt is enhancing Th17 cells differentiation, we performed the *in vitro* Th17 cells differentiation of WT and *Aim2*$^{-/-}$ in the presence or not of the RORγt activator 1b and evaluated the production of IL-17A as well as the expression of IL-1R1 and IL-23R. Interestingly, the activation of RORγt in the absence of AIM2 was associated with a decreased IL-17A expression as well as less levels of IL-1R1 and IL-23R when compared to WT Th17 cells stimulated with RORγt activator 1b and with the DMSO-stimulated controls (Figures 6F–6J). Finally, to understand the exact mechanism of the interaction between AIM2 and RORγt that drives Th17 cells differentiation, we performed chromatin immunoprecipitation (ChIP) of RORγt in WT and *Aim2*-deficient Th17 cells to analyze the RORγt-binding capacity at *Il17a* promoter region in the absence of AIM2. Interestingly, we found a compromised binding of RORγt at *Il17a* promoter region in *Aim2*-deficient Th17 cells when compared to WT Th17 cells (Figure 6K).

Taken together, these results demonstrate that during Th17 cells differentiation, AIM2 translocates to the nucleus and interacts with RORγt and enhances its binding at *Il17a* promoter which contributes to a proper Th17 cells differentiation and IL-17A production.

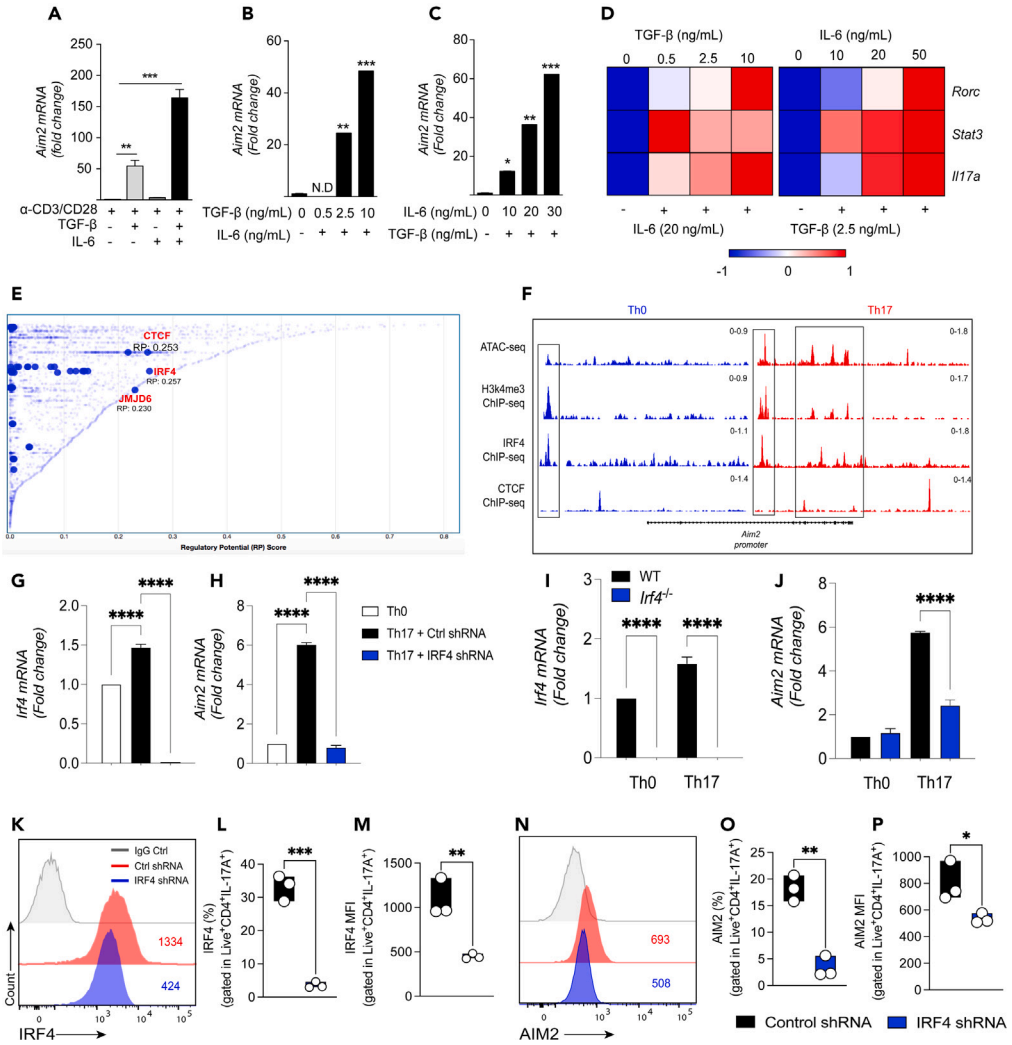

Figure 5. The expression of AIM2 in Th17 cells is regulated by IRF4

(A) AIM2 mRNA expression in activated CD4 T cells (plated with anti-CD3ε/CD28 antibodies) and in activated CD4 T cells stimulated with TGFβ or IL-6 at 36 h of culture. Fold change relative to anti-CD3ε/CD28 (n = 3).

(B) AIM2 mRNA expression in activated CD4 T cells stimulated with TGFβ (0, 0.5, 2.5, 10 ng/mL) in the presence of 20 ng/mL of IL-6. Fold change relative to TGFβ/IL-6 (0 ng/mL) (n = 3).

(C) AIM2 mRNA expression in activated CD4 T cells stimulated with IL-6 (0, 10, 20, 30 ng/mL) in the presence of 2.5 ng/mL of TGFβ. Fold change relative to TGFβ/IL-6 (0 ng/mL) (n = 3).

(D) Heatmap representing the RORC, STAT3, and IL-17A mRNA expression in activated CD4 T cells stimulated with IL-6 (0, 10, 20, 30 ng/mL) in the presence of 2.5 ng/mL of TGFβ or stimulated with TGFβ (0, 0.5, 2.5, 10 ng/mL) in the presence of 20 ng/mL of IL-6. Fold change relative to TGFβ/IL-6 (0 ng/mL) (n = 3).

(E) Regulatory potential score (RP) of transcription factors binding to AIM2 promoter in Th17 cells. Analyses were performed using the Cistrome Project platform - Cistrome DB toolkit. Available in: http://cistrome.org/db/#/.

(F) ATAC-seq analysis of the AIM2 promoter region in Th0 and Th17 cells (ID: GEO: GSM3505005/CistromeDB: 104388) (Svensson MN et al., 2019); ChIP-seq analysis of H3K4me (GEO: GSM1004818/CistromeDB: 40128), IRF4 (ID: GEO: GSM1004833/CistromeDB: 40076) and CTCF CTCF (GEO: GSM1004804/CistromeDB: 40126) at AIM2 promoter in Th0 and Th17 lymphocytes Ciofani M et al. 2012).

(G and H) IRF4 and AIM2 mRNA expression in Th0, Th17 stimulated with a control shRNA and with IRF4 shRNA (n = 3).

(I and J) IRF4 and AIM2 mRNA expression in WT and IRF4-deficient Th0 and Th17 (n = 3).

(K–P) Mean of fluorescence intensity (MFI) and frequency of IRF4 and AIM2 expression Th17 stimulated with a control shRNA and with IRF4 shRNA (n = 3). Results are considered statistically significant when $p < 0.05$, and asterisks (*) represent the level of significance according to the p value. N = 3–5. Significant differences between groups were determined by one-way ANOVA.

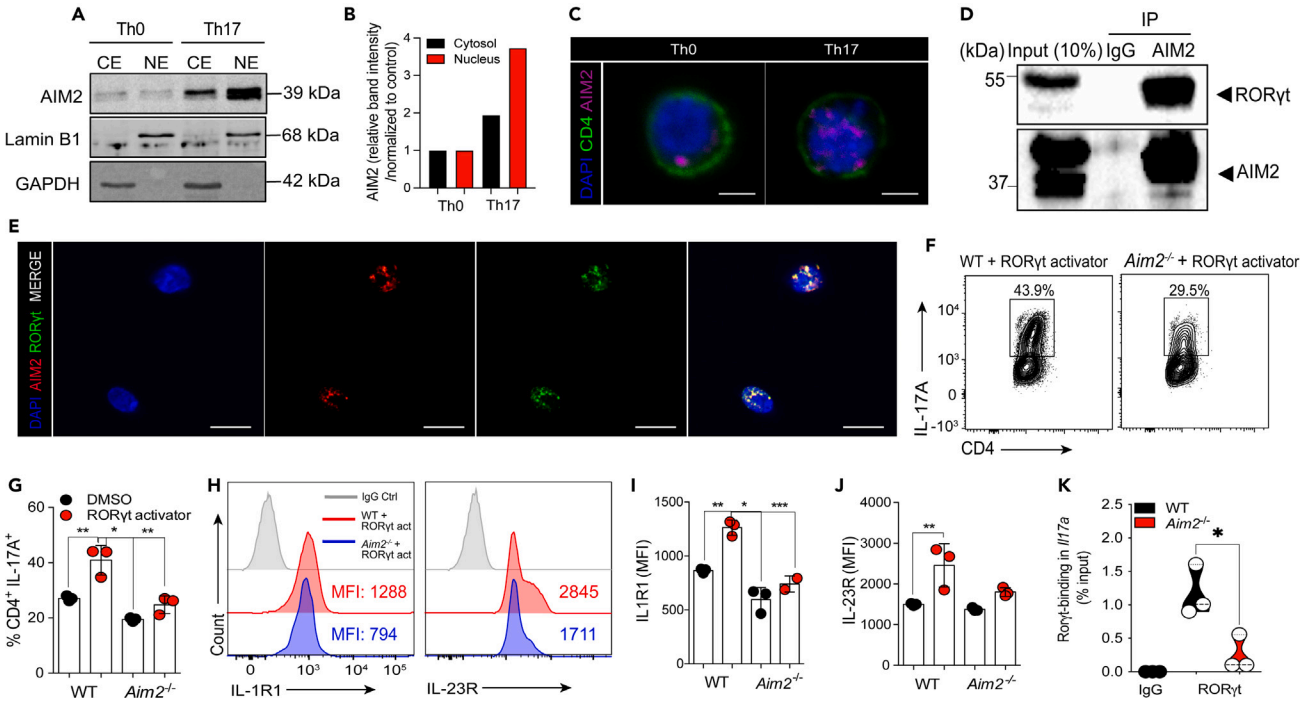

Figure 6. AIM2 promotes Th17 cell differentiation by regulating RORγt transcriptional activity

(A) Immunoblot analysis of AIM2 in cytoplasmic and nuclear fractions from Th0 and Th17 cells at 36 h of culture. Lamin B1 was used as the nuclear loading control and GAPDH was used as cytoplasmic loading control.

(B) Densitometric quantification of pro-capase-1 (C) Confocal immunofluorescence microscopy AIM2 (purple), CD4 (green) and DAPI (blue) staining in Th0 and Th17 at 36 h of culture.

(D) Immunoprecipitation of AIM2. 1x107 WT Th17 cells were differentiated and at 36 h of culture the cells were harvested, and the lysates were subjected to IP with anti-AIM2 or immunoglobulin G (IgG) control, and immunoblot of RORγt performed.

(E) Confocal immunofluorescence microscopy AIM2 (red), RORγt (green) and DAPI (blue) staining Th17 at 36 h of culture.

(F) Representative flow cytometric analysis IL-17A expression by WT and Aim2−/− Th17 cells after 96 h of culture with RORγt activator 1b. Gate strategy (Live cells+CD4+IL-17A+) (n = 3).

(G) Frequency of IL-17A and mean of fluorescence intensity (MFI) of IL-1R1 and IL-23R by WT and Aim2−/− Th17 cells after 96 h of culture with DMSO or RORγt activator 1b (n = 3).

(H–J) Representative flow cytometric analysis IL-1R1 and IL-23R expression by WT and Aim2−/− Th17 cells after 96 h of culture with RORγt activator 1b. Gate strategy (Live cells+CD4+IL-1R1+/Live cells+CD4+IL-23R+) (n = 3). (G, H, I). (K) Chromatin immunoprecipitation followed by RT-PCR (ChIP-qPCR) of RORγt-binding to the Il17a promoter region in WT and Aim2−/− Th17 cells. The data were represented as frequency of input relative to IgG control (n = 3). Data are representative of at least two independent experiments and are shown as mean ± SEM. *p < 0.05 determined by one-way ANOVA followed by Tukey's post hoc test or T-test *p < 0.05.

DISCUSSION

AIM2 plays a key role in inflammation, cancer, and host-pathogen interactions[2,5,6,19–23] Most of these studies focused on innate immune cells.[5–7] However, recent studies have pointed out that AIM2 is also an important regulator of B and T cell functions, independently of its DNA sensor function and inflammasome activation.[11,12,18,19,24] Here, we show that AIM2 is expressed both in *in vitro* and *in vivo* differentiated Th17 cells and its deficiency remarkably affects Th17 cell development and IL-17A production. In addition, AIM2 regulates the effector program of Th17 cells by augmenting the expression of RORγt, IL-1R1, and IL-23R. Accordingly, the expression of AIM2 in CD4 T cells promotes T-cell-mediated colitis development by inducing Th17 cell differentiation. Mechanistically, we show that AIM2 translocates to the nucleus and interacts with the transcription factor RORγt, enhancing its binding at the Il17a promoter region, which positively regulates Th17 cell development and IL-17A production.

In recent years, numerous studies have addressed the role of innate immune cytosolic sensors in different subtypes of CD4 T cells. Among these molecules, stand out the studies of NLRP3 in Th1, Th2, and Treg cells,[25–27] ASC,[28] caspase-1,[29] and STING[30] in Th17 cells. It was already observed that the methylation and gene expression of AIM2 in memory $CD4^+$ T cells is significantly increased when compared to naive T cells.[10] Recent studies have demonstrated that AIM2 is important for the differentiation of Treg[12,31] and follicular T cells (Tfh).[11] AIM2 is highly expressed in Tfh cells and positively regulates its differentiation by enhancing IL-21 production.[11] Although these studies point out AIM2 as an intrinsic regulator of CD4 T cell differentiation and function, the role of AIM2 in Th17 cells was not previously addressed. AIM2-deficient Treg cells exhibit impaired expression of the transcription factor FOXP3, which has been associated with increased AKT

phosphorylation and enhanced mTOR and Myc signaling. AIM2 interacts with RACK1-PP2A phosphatases in order to contain AKT phosphorylation, contributing to Tregs function.[12] A recent study found that AIM2 deficiency increases the expression of FOXP3 in Treg cells by enhancing oxidative phosphorylation and mitochondrial respiration, both of which are metabolic traits that improve Treg cell stability.[31]

We found that AIM2 is highly expressed in Th17 cells. These data agree with a previous observation by Wu and colleagues that found that AIM2 levels are increased in Th1, Th2, iTreg, Th17, and Tfh cells.[11] Furthermore, AIM2 deficiency seems to affect the production of IL-17A by CD4 T cells in experimental models of type 1 diabetes.[13] This recapitulates our findings that Aim2-deficient Th17 cells have a compromised production of IL-17A. In addition, we observe that AIM2 is required for Th17 cells differentiation during the T cell transfer colitis model. Interestingly, Rag1-deficient mice transferred with naive Aim2$^{-/-}$ CD4 T cells display less signs of colitis, which was associated with decreased frequency and number of Th17 cells and Th17 cells expressing IFN-γ in the mLNs and c-LP. Our results align with the findings of Lozano-Ruiz et al. (2022), which demonstrated the protection of Rag1−/− mice against intestinal inflammation after the transfer of Aim2−/− CD4 T cells, associated with the increased production of IL-10. Thus, it is possible that the absence of AIM2 in CD4 T cells alters the plasticity of these cells to an anti-inflammatory profile, which possibly explains the mechanisms of protection against colitis that we and Lozano-Ruiz and colleagues observed.

To find the possible mechanism by which AIM2 promotes Th17 cells differentiation, we first evaluated the canonical function of AIM2 as a DNA sensor described in innate immune cells.[5–7] Indeed, a previous study demonstrated that T cells can uptake DNA from dead cells and promote Th2 differentiation.[32] Thus, we evaluated whether such mechanisms could also occur in Th17 cells stimulated with AIM2 agonist dsDNA (poly dA:dT). However, the results of our study demonstrated that AIM2 promotes Th17 cells differentiation independently of dsDNA recognition and inflammasome activation.

The expression of AIM2 in Th17 cells is regulated by IRF4, which is an important transcription factor for Th17 cells differentiation.[15–17] Our results demonstrated that Aim2 promoter in Th17 cells is occupied by IRF4 and its deficiency is associated with decreased expression of Aim2. In line with this, Aim2-deficient Th17 cells have a compromised expression of RORγt and RORα. Moreover, the deficiency of IRF4 affects the expression of RORγt and RORα after the exposure of IL-21 [17]. Thus, this interaction between IRF4 and AIM2 could be an important factor to enhance the activity of RORγt and RORα and regulate the production of IL-17A by Th17 cells.

Because our results demonstrated that AIM2 promotes Th17 cells independently of inflammasome activation, a function that AIM2 exerts in the cytosol, we next examined the cellular localization of AIM2 in Th17 cells. Previously, it was found that, as a result of DNA damage caused by ionizing radiation and chemotherapeutic agents, AIM2 translocates to the nucleus and promotes caspase-1-dependent death of intestinal epithelial cells and bone marrow cells.[33] Similar findings were made in bone marrow (BM) cells, where nuclear AIM2 is linked to irradiation-induced BM injury by blocking DNA repair, which accelerates the production of micronuclei, genomic instability, and cell death.[34] Also in B cells, a nuclear function of AIM2 was already reported, where AIM2 translocates to the nucleus and regulates B cells differentiation in a systemic lupus erythematous experimental model.[18] Our findings, that AIM2 has a nuclear transcription-enhancing role, corroborate previous studies that showed that AIM2 can interact with Bcl-6 and Blimp-1 in B cells and enhance their differentiation to plasma cells[18] and with c-MAF in Tfh cells to promote their IL-21 production.[11]

While the cytoplasmic function of AIM2 has been well-studied, its nuclear function is still unclear. According to our study, AIM2 is necessary to enhance the binding of RORγt in the Il-17a promoter region. In addition, we observed that some genes such as Rorc, Rorα, Stat3, Il17a have a compromised expression at mRNA levels, which raises the question of whether AIM2 can directly bind to promoter regions of these genes. It is possible that the nuclear functions of AIM2 are associated with an indirect transcriptional regulation through its interaction with transcription factors or co-activators. On the other hand, AIM2 could bind to specific DNA sequences that are exposed or accessible in Th17 cells. Overall, further studies are needed to clarify the nuclear functions of AIM2.

In conclusion, we found that AIM2 acts as a critical regulator of Th17 cell differentiation by interacting with RORγt and increasing its transcription activity, thereby promoting Th17 cell development. Nonetheless, our findings clarify and support the concept of AIM2 as an intrinsic regulator of adaptive immune cells' transcriptional function. Furthermore, our findings highlight the role of AIM2 in Th17 cell-mediated intestinal inflammation, suggesting that it could be a potential therapeutic target for Th17 cell-mediated inflammatory diseases.

Our study highlights AIM2's clinical relevance in autoimmune diseases driven by Th17 cells, including rheumatoid arthritis, psoriasis, multiple sclerosis, and inflammatory bowel disease. AIM2 emerges as a potential therapeutic target to mitigate Th17 cell-mediated inflammation, with AIM2-specific inhibitors showing promise. Combining AIM2-targeted therapies with existing treatments offers synergistic possibilities. Patient stratification based on AIM2 levels may enable personalized interventions. Future preclinical and clinical investigations are needed to validate AIM2 as a therapeutic target while considering potential limitations, risks, and ethical considerations.

Limitations of the study

Our data imply that AIM2 promotes Th17 cells differentiation by interacting with RORγt and enhancing its binding at IL17a promoter. However, the major limitation of our study was the use of a full KO mice which did not allow us to explore the function of AIM2 in Th17 cells in experimental models of Th17-cell mediated disease such as EAE. In addition, further investigation is necessary to understand if AIM2 is able to bind directly to the DNA at promoter regions of genes associated with Th17 cells differentiation. We also focuses exclusively on murine models, which may not fully capture the complexity of AIM2's role in human Th17 cell differentiation, emphasizing the need for translational investigations.

STAR★METHODS

Detailed methods are provided in the online version of this paper and include the following:

- KEY RESOURCES TABLE
- RESOURCE AVAILABILITY
  - Lead contact
  - Materials availability
  - Data and code availability
- EXPERIMENTAL MODEL AND STUDY PARTICIPANT DETAILS
- METHOD DETAILS
  - *In vitro* T helper cells polarization
  - Flow cytometry (FACS)
  - Real-time PCR
  - Western blot
  - Cytoplasmic and nuclear fractionation
  - Co-immunoprecipitation assay
  - Short-hairpin RNA (shRNA) IRF4 gene silence
  - Confocal immunofluorescence microscopy
  - Model of colitis induced by adoptive transfer of CD4 T cells to $Rag1^{-/-}$ mice
  - Lamina propria cell isolation
  - Histological analysis
  - Lymphocyte proliferation and cell death assays
  - Culture of Th17 cells with AIM2 agonist (Poly dA:dT)
  - Chromatin immunoprecipitation (ChIP)
  - *In silico* analysis of public available data set of ChIP-seq and ATAC-seq
  - Cytokine quantification by ELISA
- QUANTIFICATION AND STATISTICAL ANALYSIS

SUPPLEMENTAL INFORMATION

Supplemental information can be found online at https://doi.org/10.1016/j.isci.2023.108134.

ACKNOWLEDGMENTS

We are grateful to Dr. Meire Ioshie Hiyane, Wander Ribeiro, Denise Ferraz, and Michaela Blanfeld for their technical assistance. We thank the Core Facility for Scientific Research at the University of São Paulo (CEFAP-USP/CONFOCAL/FLUIR/GENIAL) for the confocal microscopy, flow cytometry, and genome investigation analysis. The research leading to these results received funding from the São Paulo Research Foundation (FAPESP) under grant agreements 18/14815-0 to Daniela Carlos, 17/05264-7, and 2019/19435-3 (NWO FAPESP Grant) to Niels Olsen Saraiva Câmara. Ari Waisman was supported by the Deutsche Forschungsgemeinschaft (DFG, German Research Foundation) project numbers 318346496 – SFB1292/2 and 490846870 –TRR355/1. This study was also financed in part by the Coordenação de Aperfeiçoamento de Pessoal de Nível Superior – Brasil (CAPES) – Finance Code 001, which provided a scholarship to Jefferson Antônio Leite under grant agreements CAPES/PROEX: 88882.328430/2019-01 and CAPES Print/2021: 88887.575660/2020.

AUTHOR CONTRIBUTIONS

J.A.L, D.C, and N.O.S.C conceived the study. J.A.L designed and performed the experiments, analyzed data and wrote the article. L.M, E.M, C.S, A.E, L.T, T.S.R, G.C.M.C, V.Z, and A.G and helped with experiments, data analysis and discussion. M.U, D.S, F.Q.C, N.S, J.S.S, and A.W provided scientific assistance, intellectual support and critically revised the article. A.W, D.C, and N.O.S.C provided intellectual support in addition to directing and supervising the study. All authors have read and agreed to the published version of the article.

DECLARATION OF INTERESTS

The authors declare no competing financial interests.

INCLUSION AND DIVERSITY

We support inclusive, diverse, and equitable conduct of research.

Received: June 7, 2023
Revised: September 15, 2023
Accepted: October 2, 2023
Published: October 4, 2023

REFERENCES

1. Dawson, M.J., and Trapani, J.A. (1996). HIN-200, a novel family of IFN-inducible nuclear proteins expressed in leukocytes. J. Leukoc. Biol. *60*, 310–316. https://doi.org/10.1002/jlb.60.3.310.
2. Trent, J.M., Stanbridge, E.J., McBride, H.L., Meese, E.U., Casey, G., Araujo, D.E., Witkowski, C.M., and Nagle, R.B. (1990). Tumorigenicity in human melanoma cell lines controlled by introduction of human chromosome 6. Science *247*, 568–571. https://doi.org/10.1126/science.2300817.
3. DeYoung, K.L., Ray, M.E., Su, Y.A., Anzick, S.L., Johnstone, R.W., Trapani, J.A., Meltzer, P.S., and Trent, J.M. (1997). Cloning a novel member of the human interferon-inducible gene family associated with control of tumorigenicity in a model of human melanoma. Oncogene *15*, 453–457. https://doi.org/10.1038/sj.onc.1201206.
4. Choubey, D., Walter, S., Geng, Y., and Xin, H. (2000). Cytoplasmic localization of the interferon-inducible protein that is encoded by the AIM2 (absent in melanoma) gene from the 200-gene family. FEBS Lett. *474*, 38–42. https://doi.org/10.1016/S0014-5793(00)01571-4.
5. Hornung, V., Ablasser, A., Charrel-Dennis, M., Bauernfeind, F., Horvath, G., Caffrey, D.R., Latz, E., and Fitzgerald, K.A. (2009). AIM2 recognizes cytosolic dsDNA and forms a caspase-1-activating inflammasome with ASC. Nature *458*, 514–518. https://doi.org/10.1038/nature07725.
6. Fernandes-Alnemri, T., Yu, J.W., Datta, P., Wu, J., and Alnemri, E.S. (2009). AIM2 activates the inflammasome and cell death in response to cytoplasmic DNA. Nature *458*, 509–513. https://doi.org/10.1038/nature07710.
7. Roberts, T.L., Idris, A., Dunn, J.A., Kelly, G.M., Burnton, C.M., Hodgson, S., Hardy, L.L., Garceau, V., Sweet, M.J., Ross, I.L., et al. (2009). HIN-200 proteins regulate caspase activation in response to foreign cytoplasmic DNA. Science *323*, 1057–1060. https://doi.org/10.1126/science.1169841.
8. Eichholz, K., Bru, T., Tran, T.T.P., Fernandes, P., Welles, H., Mennechet, F.J.D., Manel, N., Alves, P., Perreau, M., and Kremer, E.J. (2016). Immune-Complexed Adenovirus Induce AIM2-Mediated Pyroptosis in Human Dendritic Cells. PLoS Pathog. *12*, e1005871. https://doi.org/10.1371/journal.ppat.1005871.
9. Costa Franco, M.M.S., Marim, F.M., Alves-Silva, J., Cerqueira, D., Rungue, M., Tavares, I.P., and Oliveira, S.C. (2019). AIM2 senses Brucella abortus DNA in dendritic cells to induce IL-1β secretion, pyroptosis and resistance to bacterial infection in mice. Microbes Infect. *21*, 85–93. https://doi.org/10.1016/j.micinf.2018.09.001.
10. Komori, H.K., Hart, T., LaMere, S.A., Chew, P.V., and Salomon, D.R. (2015). Defining CD4 T Cell Memory by the Epigenetic Landscape of CpG DNA Methylation. J. Immunol. *194*, 1565–1579. https://doi.org/10.4049/jimmunol.1401162.
11. Wu, H., Deng, Y., Long, D., Yang, M., Li, Q., Feng, Y., Chen, Y., Qiu, H., Huang, X., He, Z., et al. (2022). The IL-21-TET2-AIM2-c-MAF pathway drives the T follicular helper cell response in lupus-like disease. Clin. Transl. Med. *12*, e781. https://doi.org/10.1002/CTM2.781.
12. Chou, W.C., Guo, Z., Guo, H., Chen, L., Zhang, G., Liang, K., Xie, L., Tan, X., Gibson, S.A., Rampanelli, E., et al. (2021). AIM2 in regulatory T cells restrains autoimmune diseases. Nature *591*, 300–305. https://doi.org/10.1038/s41586-021-03231-w.
13. Leite, J.A., Pessenda, G., Guerra-Gomes, I.C., de Santana, A.K.M., André Pereira, C., Ribeiro Campos Costa, F., Ramos, S.G., Simões Zamboni, D., Caetano Faria, A.M., Candido de Almeida, D., et al. (2020). The DNA Sensor AIM2 Protects against Streptozotocin-Induced Type 1 Diabetes by Regulating Intestinal Homeostasis via the IL-18 Pathway. Cells *9*. https://doi.org/10.3390/cells9040959.
14. Liu, T., Ortiz, J.A., Taing, L., Meyer, C.A., Lee, B., Zhang, Y., Shin, H., Wong, S.S., Ma, J., Lei, Y., et al. (2011). Cistrome: an integrative platform for transcriptional regulation studies. Genome Biol. *12*, R83. https://doi.org/10.1186/GB-2011-12-8-R83.
15. Brüstle, A., Heink, S., Huber, M., Rosenplänter, C., Stadelmann, C., Yu, P., Arpaia, E., Mak, T.W., Kamradt, T., and Lohoff, M. (2007). The development of inflammatory T(H)-17 cells requires interferon-regulatory factor 4. Nat. Immunol. *8*, 958–966. https://doi.org/10.1038/NI1500.
16. Mudter, J., Yu, J., Zufferey, C., Brüstle, A., Wirtz, S., Weigmann, B., Hoffman, A., Schenk, M., Galle, P.R., Lehr, H.A., et al. (2011). IRF4 regulates IL-17A promoter activity and controls RORγt-dependent Th17 colitis *in vivo*. Inflamm. Bowel Dis. *17*, 1343–1358. https://doi.org/10.1002/IBD.21476.
17. Huber, M., Brüstle, A., Reinhard, K., Guralnik, A., Walter, G., Mahiny, A., von Löw, E., and Lohoff, M. (2008). IRF4 is essential for IL-21-mediated induction, amplification, and stabilization of the Th17 phenotype. Proc. Natl. Acad. Sci. USA *105*, 20846–20851. https://doi.org/10.1073/PNAS.0809077106.
18. Yang, M., Long, D., Hu, L., Zhao, Z., Li, Q., Guo, Y., He, Z., Zhao, M., Lu, L., Li, F., et al. (2021). AIM2 deficiency in B cells ameliorates systemic lupus erythematosus by regulating Blimp-1–Bcl-6 axis-mediated B-cell differentiation. Signal Transduct. Target. Ther. *6*, 341. https://doi.org/10.1038/s41392-021-00725-x.
19. El-Zaatari, M., Bishu, S., Zhang, M., Grasberger, H., Hou, G., Haley, H., Humphries, B., Syu, L.J., Dlugosz, A.A., Luker, K., et al. (2020). Aim2-mediated/IFN-β-independent regulation of gastric metaplastic lesions via CD8+ T cells. JCI Insight *5*, e94035. https://doi.org/10.1172/jci.insight.94035.
20. Saiga, H., Kitada, S., Shimada, Y., Kamiyama, N., Okuyama, M., Makino, M., Yamamoto, M., and Takeda, K. (2012). Critical role of AIM2 in Mycobacterium tuberculosis infection. Int. Immunol. *24*, 637–644. https://doi.org/10.1093/INTIMM/DXS062.
21. Ma, C., Li, S., Hu, Y., Ma, Y., Wu, Y., Wu, C., Liu, X., Wang, B., Hu, G., Zhou, J., and Yang, S. (2021). AIM2 controls microglial inflammation to prevent experimental autoimmune encephalomyelitis. J. Exp. Med. *218*, e20201796. https://doi.org/10.1084/JEM.20201796.
22. Hu, S., Peng, L., Kwak, Y.T., Tekippe, E.M., Pasare, C., Malter, J.S., Hooper, L.V., and Zaki, M.H. (2015). The DNA Sensor AIM2 Maintains Intestinal Homeostasis via Regulation of Epithelial Antimicrobial Host Defense. Cell Rep. *13*, 1922–1936. https://doi.org/10.1016/J.CELREP.2015.10.040.
23. Rathinam, V.A.K., Jiang, Z., Waggoner, S.N., Sharma, S., Cole, L.E., Waggoner, L., Vanaja, S.K., Monks, B.G., Ganesan, S., Latz, E., et al. (2010). The AIM2 inflammasome is essential for host defense against cytosolic bacteria and DNA viruses. Nat. Immunol. *11*, 395–402. https://doi.org/10.1038/NI.1864.
24. Svensson, A., Patzi Churqui, M., Schlüter, K., Lind, L., and Eriksson, K. (2017). Maturation-dependent expression of AIM2 in human B-cells. PLoS One *12*, e0183268. https://doi.org/10.1371/journal.pone.0183268.
25. Arbore, G., West, E.E., Spolski, R., Robertson, A.A.B., Klos, A., Rheinheimer, C., Dutow, P., Woodruff, T.M., Yu, Z.X., O'Neill, L.A., et al. (2016). T helper 1 immunity requires complement-driven NLRP3 inflammasome activity in $CD4^+$ T cells. Science *352*, aad1210. https://doi.org/10.1126/SCIENCE.AAD1210.
26. Bruchard, M., Rebé, C., Derangère, V., Togbé, D., Ryffel, B., Boidot, R., Humblin, E., Hamman, A., Chalmin, F., Berger, H., et al. (2015). The receptor NLRP3 is a transcriptional regulator of TH2 differentiation. Nat. Immunol. *16*, 859–870. https://doi.org/10.1038/ni.3202.
27. Park, S.H., Ham, S., Lee, A., Möller, A., and Kim, T.S. (2019). NLRP3 negatively regulates Treg differentiation through Kpna2-mediated nuclear translocation. J. Biol. Chem. *294*, 17951–17961. https://doi.org/10.1074/JBC.RA119.010545.
28. Martin, B.N., Wang, C., Zhang, C.J., Kang, Z., Gulen, M.F., Zepp, J.A., Zhao, J., Bian, G., Do, J.S., Min, B., et al. (2016). T cell-intrinsic ASC critically promotes T H 17-mediated experimental autoimmune encephalomyelitis. Nat. Immunol. *17*, 583–592. https://doi.org/10.1038/ni.3389.
29. Gao, Y., Deason, K., Jain, A., Irizarry-Caro, R.A., Dozmorov, I., Coughlin, L.A., Rauch, I., Evers, B.M., Koh, A.Y., Wakeland, E.K., and Pasare, C. (2020). Transcriptional profiling identifies caspase-1 as a T cell-intrinsic regulator of Th17 differentiation. J. Exp. Med. *217*, e20190476. https://doi.org/10.1084/JEM.20190476.
30. Alves Damasceno, L.E., Cesar, G., Cebinelli, M., Cunha, M., Cunha, F.Q., and Alves-Filho, C. (2022). STING Is an Intrinsic Checkpoint Inhibitor that Restrains the T H 17 Cell Pathogenic Program. https://doi.org/10.1016/j.celrep.2022.110838.
31. Lozano-Ruiz, B., Tzoumpa, A., Martínez-Cardona, C., Moreno, D., Aransay, A.M.,

Cortazar, A.R., Picó, J., Peiró, G., Lozano, J., Zapater, P., et al. (2022). Absent in Melanoma 2 (AIM2) Regulates the Stability of Regulatory T Cells. Int. J. Mol. Sci. *23*, 2230. https://doi.org/10.3390/IJMS23042230/S1.

32. Imanishi, T., Ishihara, C., Badr, M.E.S.G., Hashimoto-Tane, A., Kimura, Y., Kawai, T., Takeuchi, O., Ishii, K.J., Taniguchi, S., Noda, T., et al. (2014). Nucleic acid sensing by T cells initiates Th2 cell differentiation. Nat. Commun. *5*, 3566. https://doi.org/10.1038/ncomms4566.

33. Hu, B., Jin, C., Li, H.B., Tong, J., Ouyang, X., Cetinbas, N.M., Zhu, S., Strowig, T., Lam, F.C., Zhao, C., et al. (2016). The DNA-sensing AIM2 inflammasome controls radiation-induced cell death and tissue injury. Science *354*, 765–768. https://doi.org/10.1126/SCIENCE.AAF7532.

34. Jiang, H., Swacha, P., and Gekara, N.O. (2021). Nuclear AIM2-Like Receptors Drive Genotoxic Tissue Injury by Inhibiting DNA Repair. Adv. Sci. *8*, 2102534. https://doi.org/10.1002/ADVS.202102534.

STAR★METHODS

KEY RESOURCES TABLE

REAGENT or RESOURCE	SOURCE	IDENTIFIER
Antibodies		
anti-mouse CD4	BD Biosciences	Cat#100432; GK1.5; AB_10013429
Anti-mouse CD62L	Biolegend	Cat#104405; MEL-14; AB_976598
anti-mouse CD45	Biolegend	Cat#103138; 30-F11; AB_2563061
Anti-mouse TCR-β	Biolegend	Cat#109207; AB_313430
Anti-mouse IL-17A	eBioscience	Cat#11-7177; eBio17B7; AB_925754
Anti-mouse IFNy	eBioscience	Cat#25-7311; XMG1.2; AB_465411
Anti-mouse RORyt	BD Biosciences	Cat#562894; Q31-378; AB_2687545
Anti-mouse FOXP3	eBioscience	Cat#17-5773; FJK-16s; AB_465243
Anti-mouse IL-1R1	Biolegend	Cat#113509; JAMA-147; AB_566478
Anti-mouse IL-23R	Biolegend	Cat#516803; O78-1208; AB_2738972
Anti-human/mouse AIM2	BD Biosciences	Cat#652803; 2B10; AB_2566000
Anti-mouse IRF4	eBioscience	Cat#46-9858-82; 3E4; AB_2573912
Anti-mouse GAPDH	Cell Signaling	Cat#97166; AB_2756824
Anti-mouse AIM2	Cell Signaling	Cat#63660; AB_2890193
Anti-mouse RORyt	Abcam	Cat#Ab113434; AB_10860312
Anti-mouse CD3ε	BD Biosciences	Cat#553058; 145-2C11; AB_394591
Anti-mouse CD28	BD Biosciences	Cat#553294;37.51 RUO; AB_394763
Anti-mouse IFNy	BD Biosciences	Cat#554408; XMG-1.2; AB_395373
Anti-mouse IL-4	BD Biosciences	Cat#554432; 11B11; AB_395388
Anti-mouse IL-2	BD Biosciences	Cat#554424; JES6-1A12; AB_395383
Mouse Anti-GAPDH (clone D4C6R)	*Cell Signaling*	*Cat# 97166; AB_2756824*
Anti-mouse lamin-B1 (Clone D4Q4Z)	*Cell Signaling*	Cat#12586; AB_2650517
Chemicals, peptides, and recombinant proteins		
Murine recombinant TGFβ	R&D systems	Cat#7666-MB
Murine recombinant IL-6	Peprotech	Cat#216-16
Murine recombinant IL-23	R&D systems	Cat#1887-ML
Murine recombinant IL-1β	Peprotech	Cat# 211-11B
Murine recombinant IL-12	Peprotech	Cat#212-12
Murine recombinant IL-4	Peprotech	Cat#214-14
CollagenaseTypeVIII	*Sigma-Aldrich*	Cat#C2139
FBS	Gibco	Lot.1640960
HyCloneTM Fetal Bovine Serum	*GE Healthcare*	*Cat# SV30160.03*
CD4 (L3T4) MicroBeads, mouse	*Miltenyi Biotec*	*Cat# 130-117-043*
Laemmli sample buffer	*Bio-Rad*	*Cat# 161-0737*
Trans-Blot Turbo Mini Nitrocellulose Transfer Packs	*Bio-Rad*	*Cat #1704158*
b-Mercaptoethanol	*Sigma-Aldrich*	*Cat# M6250*
IMDM (Iscove's Modification of DMEM)	*Corning*	*Cat# 15-016*
L-Glutamine	*Corning*	*Cat# 25-005*
Penicillin-Streptomycin	*Sigma-Aldrich*	*Cat# P4333*
Foxp3/Transcription Factor Staining Buffer Set	*Invitrogen*	*Cat# 00-5523-00*

(*Continued on next page*)

Continued

REAGENT or RESOURCE	SOURCE	IDENTIFIER
Bovine serum albumin (BSA)	*Sigma-Aldrich*	*Cat# A9418*
Power SYBR Green Master Mix	*Applied Biosystems*	*Cat# 4368708*
PMA	*Sigma-Aldrich*	*Cat# P1585*
Ionomycin	*Sigma-Aldrich*	*Cat# I0634*
Brefeldin A	Biolegend	*Cat# 420601*
Protease/Phosphatase Inhibitor Cocktail (100X)	*Cell Signaling*	*Cat# 5872*
ECL Prime	*GE Healthcare*	*Cat# RPN2236*
RPMI1640	*ThermoFisher*	*Cat#21875158*
HEPES	*ThermoFisher*	*Cat#15630130*
DNaseI	*Sigma-Aldrich*	*Cat#11284932001*
Critical commercial assays		
RNA Isolation RNeasy Mini Kit	*QIAGEN*	*Cat# 74104*
Bicinchoninic Acid (BCA) kit for Protein Determination	*Sigma-Aldrich*	*Cat# BCA1*
PierceTM Co-Immunoprecipitation Kit	*Thermo Scientific*	*Cat# 26149*
High-Capacity cDNA Reverse Transcription Kit	*Applied Biosystems*	*Cat# 4368813*
ChIP-IT High Sensitivity	Active motif	53040
Experimental models: Organisms/strains		
Mouse: C57BL/6	*The Jackson Laboratory*	*N/A*
Mouse: AIM2KO	(Jones et al., 2010)	N/A
Mouse: IRF4KO	(Huber et al., 2008)	N/A
Oligonucleotides		
Aim2 fwd: 5′-TCTGTCCTCAAGCTAAGCCTCA-3′ Aim2 rev: 5′- GTGACAACAAGTGGATCTTTCTGTA-3′	*ThermoFisher*	N/A
Rorc fwd: 5′- GAGTTTGCCAAGCGGCTTT-3′ Rorc rev: 5′- TCCATTGCTCCTGCTTTCAGTACA-3′	*ThermoFisher*	N/A
Rorα fwd: 5′- TGGTTGAAGGATGTTCCACA-3′ *Rorα rev: 5′*- TGGTTG AAGGATGTTCCACA-3′	*ThermoFisher*	N/A
Stat3 fwd: 5′-AGGAGTCTAACAACGGCAGCCT-3′ Stat3 rev: 5′- GTGGTACACCTCAGTCTCGAA-3′	*ThermoFisher*	N/A
Foxp3 fwd: 5′- TTCTCCAGGACAGACCACACT-3′ Foxp3 rev: 5′- TTCTCCAGGACAGACCACACT-3′	*ThermoFisher*	N/A
Il23r fwd: 5′- GCCAAGAAGACCATTCCCGA-3′ Il23r rev: 5′- TCAGTGCTACAATCTTCTTCAGAGG-3′	*ThermoFisher*	N/A
Il1r1 fwd: 5′- AAGCTGACCCAGGATCAATG-3′ Il1r1 rev: 5′- TGGTTGAAGGATGTTCCACA-3′	*ThermoFisher*	N/A
Il17r fwd: 5′- CTGTATGACCTGGAGGCTTTCT-3′ Il17r rev: 5′- CGAGTAGACGATCCAGACCTTC-3′	*ThermoFisher*	N/A
Il17a fwd: 5′-GCTCCAGAAGGCCCTCAG-3′ *Il17a rev: 5′*- CTTTCCCTCCGCATTGACA-3′	*ThermoFisher*	N/A
Il22 fwd: 5′- CAGCTCCTGTCACATCAGCGGT-3′ *Il22 rev: 5*- AGGTCCAGTTCCCCAATCGCCT-3′	*ThermoFisher*	N/A
Gapdh fwd: 5′-CATCTTCTTGTGCAGTGCCA-3′ *Gapdh rev: 5′*- CGGCCAAATCCGTTCAC-3′	*ThermoFisher*	N/A
Il17a promoter fwd: 5′-CACCTCACACGAGGCACAAG-3′ *Il17a promoter rev: 5′*-ATGTTTGCGCGTCCTGATC-3′	*ThermoFisher*	N/A

(*Continued on next page*)

Continued

REAGENT or RESOURCE	SOURCE	IDENTIFIER
Software and algorithms		
BD FACSDiva software	*BD Biosciences*	N/A
FlowJo v10	*BD Biosciences*	https://www.flowjo.com
Morpheus	*Broad Institute*	https://software.broadinstitute.org/morpheus/
Prism 8	*GraphPad*	https://www.graphpad.com
Other		
IRF4 shRNA	Santa Cruz Biotechnology	sc-35713-V
scramble shRNA	Santa Cruz Biotechnology	sc-108060

RESOURCE AVAILABILITY

Lead contact

Further information and requests for reagents and resources should be directed to and will be fulfilled by the lead contacts, Niels Olsen Saraiva Câmara (niels@icb.usp.br).

Materials availability

This study did not generate new unique reagents.

Data and code availability

- Data: This paper does not generated sequencing data. Microrray, ATAC-seq and ChIP-seq data was reanalyzed based on public datasets available on Gene Expression Omnibus(GEO). The accession number is available on the STAR Methods section of this paper.
- Code: This paper does not report original code.
- Other items: No other new unique reagent was generated. Any additional information required to reanalyze the data reported in this paper is available from the lead contact upon request.

EXPERIMENTAL MODEL AND STUDY PARTICIPANT DETAILS

Male wild-type C57BL/6, Aim2-/- and IRF4-/- mice aged 6-10 weeks and weighing 20-25 grams were used. The AIM2-/- mice were obtained from Genentech, South San Francisco, CA, with the lineage name Aim2tm1.2Arte. All procedures were performed in accordance with the principles proposed by the Brazilian College of Animal Experimentation (COBEA) and approved by the Ethics Committee on Animal Experimentation of the University of São Paulo (CEUA/FMRP: 124/2020; ICB: 7035150721).

METHOD DETAILS

In vitro T helper cells polarization

In vitro T helper cells polarization was performed by isolating naïve $CD4^+$ T cells from the spleen and lymph nodes of WT and Aim2-/- mice using microbeads coated with anti-CD4 (clone L3T4, cat 130-117-043, Miltenyi Biotec, Bergisch Gladbach, Germany). The cells were then stained with fluorochrome-conjugated anti-CD4, anti-CD44, and anti-CD62L antibodies, and $CD4^+CD44^{low}CD62L^{high}$ cells were isolated by sorting (FACS Aria III sorter, BD Biosciences). For the differentiation, the CD4 T cells obtained from the sorting were placed in 48-well plates coated with anti-CD3 (2 ug/mL – BD Bioscience Cat. 553058, Clone – 145-2C11) anti-CD28 (1 ug/mL - BD Bioscience Cat. 553294, Clone: 37.51 RUO), and subsequently stimulated with a cocktail of cytokines and neutralizing antibodies. Th17: 2.5 ng/mL of TGF-beta (R&D – Cat. 7666MB), 50 ng/mL of IL-6 (Peprotech – Cat. 216-16), 50 ng/mL of IL-23 (R&D, Cat. 1887-ML), 20 ng/mL of IL-1beta (Peprotech, Cat. 211-11B) and 1 ug/mL of anti-IFNg (BD Bioscience, Cat. 554408) , IL-4 (BD Bioscience, Cat. 554432, Clone: 11B11) and IL-2 (BD Bioscience, Cat. 554424, Clone: JES6-1A12). Th1: 20 ng/mL of IL-12 (Cat. 212-12, Peprotech) and 1 ug/mL anti-IL-4 (Cat. 554432, BD Bioscience). Th2: 10 ng/mL of IL-4 (Cat. 214-14, Peprotech) and and 1 ug/mL of anti-IFNg (BD Bioscience, Cat. 554408). iTreg: 10 ng/mL TGF-beta (R&D – Cat. 7666MB) and and 1 ug/mL of anti-IFNg (BD Bioscience, Cat. 554408).

Flow cytometry (FACS)

Quantitative and phenotypic analysis of cells differentiated *in vitro* or isolated from lymph nodes, spleen, or intestinal lamina propria was performed by flow cytometry. Briefly, after being isolated, cells were counted and evaluated for viability with trypan blue. Subsequently, the cells were plated in a 96-well plate and stimulated with phorbol myristate acetate (PMA) (50 ng/ml; Sigma Aldrich) and ionomycin (500 ng/ml; Sigma Aldrich), and brefeldin A (transport inhibitor of golgi - 1.5 μl/ml; BD Biosciences), for 4 hours in an oven at 37°C (5% CO2 and 8%

humidity). The number of cells used were 5x10^5/cells per well for experiments derived from *in vitro* culture of lymphocytes or 2x10^6/cells per well for *in vivo* experiments. Then, the cells were washed twice with PBS 1x and centrifuged at 450 g for 5 minutes and incubated for 15 minutes with Fc block (1:200) to block Fc receptors, and subsequently washed with PBS 1x, centrifuged at 450 g per 5 and stained with cell viability marker (Fixable viability dye; 1:1000; eBioscience) and anti-CD4 (1:200; BD Biosciences) for 10 minutes at room temperature. Then, the cells were centrifuged and fixed using the kit's fixative (transcription factor staining buffer set, eBioscience) for 60 minutes at room temperature, with subsequent centrifugation. The next step was intracellular labeling with antibodies listed in for 60 minutes. Briefly, the antibodies were diluted in the kit's permeabilizer, and the cells were incubated with permeabilization buffer containing the antibody mix for 60 minutes at 4°C. After this step, the cells were centrifuged again and resuspended in PBS for acquisition by flow cytometry (FACS Canto II, BD Biosciences). In this step, between 100,000 and 250,000 events were acquired according to the experiment. Sample analyses were performed using the FlowJo X software (BD Biosciences).

Real-time PCR

To assess gene expression of Th17 cell cultures, cells were harvested, and RNA was extracted using the RNA Extraction Kit (Promega) according to the manufacturer's instructions. After extraction, samples were quantified using a nanodrop (ThermoFisher) and 500 ng of RNA were converted to cDNA using the High-Capacity cDNA Reverse Transcription Kit (ThermFisher), according to the manufacturer's instructions. Real-time PCR reactions were performed using cDNA, primers, and the Sybr Green Master Mix containing reaction products such as nucleotides and polymerase. The reactions were performed with the StepOnePlus device (ThermoFisher). The results were analyzed using the cycle threshold (CT), with the data normalized by the Gapdh expression and the difference between the groups calculated using the 2-ΔΔCT method. The sequences of the primers used are described in the table below. None of the primers used showed amplification in the group without sample (blank) or more than one peak in the melting curve. In addition, all primers showed an efficiency greater than 90%.

Western blot

To evaluate AIM2 protein expression, samples were collected in RIPA buffer (Sigma Aldrich), homogenized with protease, centrifuged, and the supernatant collected. Then, protein quantification was performed using the Bicinchoninic acid protein assay (BCA; Sigma Aldrich). For the experiments with samples of CD4 T cells, 30 μg of proteins were used. Sample preparation was performed with 2x Laemmli sample buffer (Bio-rad), and heated for 10 minutes at 95°C for protein denaturation. Subsequently, the samples were applied to a 12% gradient polyacrylamide gel (Bio-rad) and, after separation, were transferred to 0.2 μm nitrocellulose membranes (Bio-rad), through the Trans-Blot Turbo transfer system (Bio-rad). Then, the membranes were blocked in TBST (TRIS-HCl 100 mM pH 7.5, NaCl 150 mM, Tween20 0.05%) with 5% milk (Cell Signaling) to reduce nonspecific binding, washed with TBST and incubated with the primary antibodies diluted in 5% TBST BSA (Sigma Aldrich), overnight, at 4°C under slow agitation. Then, the membranes were washed and secondary antibodies (anti-rabbit AIM2 Cat. #63660, Cell signaling) were added in TBST with 5% milk (Cell Signaling), for 2 hours at room temperature and slow stirring. Subsequently, the membranes were washed for 30 minutes with TBST and the substrate Luminata (Millipore) was added for chemiluminescence detection, using the ChemiDocTM XRS equipment (Bio-rad) and analyzed with the Image Lab 3.0 program (Bio-rad). An anti-GAPDH antibody (#97166 Cell Signaling) was used as a protein loading control.

Cytoplasmic and nuclear fractionation

To evaluate the location of AIM2 in CD4 T cells, 1x10^7 Th0 and Th17 cells were collected after 36 hours of culture and cytoplasmic and nuclear separation was performed using the NE-PER™ Nuclear and Cytoplasmic Extraction Reagents (Cat. 78833) according to the manufacturer's instructions. After fractionation of the cytoplasm and nucleus, the samples were quantified by the BCA method and placed in 2x Laemmli sample buffer (Bio-rad) for further protein denaturation, as described above. The subsequent steps were like a Western blot. Lamin B1 was used as a nuclear protein loading control and GAPDH was used as a cytoplasmic protein loading control.

Co-immunoprecipitation assay

Immunoprecipitation was performed using the Pierce CO-IP Kit (Thermo Scientific) following the manufacturer's protocol. In this experiment, 1x107 cells per IP were used. Briefly, control IgG antibodies (Cat. #2729, Cell Signaling) and mouse anti-AIM2 (Cat. #63660, Cell Signaling) were immobilized using AminoLink Plus coupling resin. Equal amounts of Th17 cell lysates were pre-cleaned and subsequently incubated with the antibody-coupled resin overnight at 4°C. Subsequently, the resin was washed, and the proteins eluted with an elution buffer. Immunoprecipitated samples were analyzed for expression of RORγt protein (Cat. Ab113434, Abcam) and AIM2 by immunoblotting.

Short-hairpin RNA (shRNA) IRF4 gene silence

$5x10^5$ WT CD4 T cells were culture in Th0 and Th17 cells condition as describe above and in the presence of IRF4 shRNA (Santa Cruz Biotechnology, sc-35713-V) or a scramble shRNA (Santa Cruz Biotechnology, sc-108060). After 48h of culture, the cells was collect and the knockdown of IRF4 and AIM2 expression was accessed by qPCR and flow cytometry.

Confocal immunofluorescence microscopy

For immunofluorescence, Th0 or Th17 cells obtained from cultures were collected, fixed, and permeabilized on slides. Subsequently, the preparations were incubated with primary anti-AIM2, anti-CD4, and anti-RORgt antibodies followed by the addition of fluorophore-conjugated secondary antibodies (AF488, AF594, and AF647). Finally, the cover slips were introduced onto the slides together with the mounting medium Prolong® Gold Antifade Reagent with DAPI (nuclear labeling). Images were captured by a Leica TCS SP5 confocal microscope and analyzed using ImageJ software.

Model of colitis induced by adoptive transfer of CD4 T cells to Rag1$^{-/-}$ mice

$CD4^{+}CD45RB^{high}$ T cells (2.5 x 10^6) were isolated by sorting from lymph node and spleen samples of WT and Aim2-/- mice, and subsequently 5 x 10^5 cells were injected intraperitoneally into Rag1-/- mice. The mice that received the cells had their weight monitored daily, and in week zero and in the fourth week after the transfer they were anesthetized and submitted to a microendoscopy procedure to evaluate inflammation in the colon. After 8 weeks, the animals were euthanized and the mesenteric lymph nodes (LNM), spleen, and colon were collected for flow cytometry and H&E analyses.

Lamina propria cell isolation

Intestines removed from euthanized animals were opened lengthwise, washed with PBS to remove feces, and cut into pieces approximately 1 cm in size. The pieces were then incubated with RPMI medium containing 3% fetal bovine serum, EDTA, and DTT for 20 minutes at 37°C with agitation. After incubation, the pieces of intestine were sieved and washed with medium containing EDTA to separate the intraepithelial lymphocytes. The solution resulting from the washes, which contained the intraepithelial lymphocytes, was discarded. The remaining pieces were then digested with medium containing liberase (1/250 of a 25 mg/mL solution, Roche, Germany) and DNAse I (Sigma-Aldrich, St. Louis, MO, USA) for 25 minutes at 37°C with agitation. After digestion, the solution was passed through a sieve (70 μm), centrifuged, resuspended in PBS + 2% FBS, and passed again through a sieve (40 μm). The lamina propria cells obtained were then marked with monoclonal antibodies for analysis of the marking of surface and intracellular molecules, according to the cell population to be analyzed.

Histological analysis

A large intestinal fragment was removed, fixed in metacarn (60% Methanol, 30% Chloroform, and 10% Glacial Acetic Acid) for 24 hours at 4°C and subsequently transferred to a 70% alcohol solution. The material was sent for mounting in paraffin blocks and the prepared slides were stained with H&E (Hematoxylin & Eosin). Images were obtained using a Nikon microscope at 10x, 20x, and 40x. The histology score analysis was performed according to the guidance for scoring colonic inflammation mediated by disturbed immune cell homeostasis published by Erban et al. (2014).

Lymphocyte proliferation and cell death assays

WT and Aim2-/- Th17 cells were differentiated for 96 hours, and the proliferation index was evaluated using carboxyfluorescein succinimidyl ester (CFSE) dilution (Sigma), and apoptosis was evaluated by Annexin V staining (BD Biosciences).

Culture of Th17 cells with AIM2 agonist (Poly dA:dT)

WT and Aim2-/- Th17 cells were differentiated in the presence of Poly dA:dT for 96 hours. After the incubation period with the specific stimulus, the cells and the supernatant were collected for further analysis of active caspase-1 and measurement of cytokines IL-17A and IL-1β.

Chromatin immunoprecipitation (ChIP)

WT and Aim2-/- Th17 cells were differentiated and at 96 h of culture were crosslinked by fixation with 1.1% paraformaldehyde for 10 min at room temperature. Sonicated chromatin from 2.5x10^6 cells was subjected to ChIP using the Imprint Chromatin Immunoprecipitation Kit (Sigma-Aldrich, Cat. CHP1). Chromatin was incubated in a pre-coated strip well with 5 μg/mL of rabbit anti-RORgt (Santa Cruz Biotechnology Cat#: sc-28559) or normal rabbit IgG. Next, the crosslinks were reversed, and the DNA was purified by spin column cleanup. qRT-PCR was performed on DNA recovered from IP and input samples.

In silico analysis of public available data set of ChIP-seq and ATAC-seq

ChiP-seq and ATAC-seq analysis of public data set was analysed using the Cistrome Project.[14] Regulatory potential score (RP) of transcription factors binding to AIM2 promoter in Th17 cells were performed using the Cistrome Project platform - Cistrome DB toolkit available in: http://cistrome.org/db/#/. ATAC-seq analysis of the AIM2 promoter region in Th0 and Th17 cells (ID: GEO: GSM3505005/CistromeDB: 104388) (Svensson MN et al., 2019). ChIP-seq analysis of H3K4me3 (GEO: GSM1004818/CistromeDB: 40128), IRF4 (ID: GEO: GSM1004833/CistromeDB: 40076) and CTCF CTCF (GEO: GSM1004804/CistromeDB: 40126) at AIM2 promoter in Th0 and Th17 cells Ciofani M et al. 2012). ChIP-seq analysis of the transcription factors STAT3 (GEO: GSM1004866/CistromeDB: 40113), BATF (GEO: GSM1004833/CistromeDB: 40076), c-MAF (GEO: GSM1004799/CistromeDB: 40143), p-300 (GEO: GSM1004852/CistromeDB: 40123), JMJD6 (GEO: GSM1004840/CistromeDB: 40095), FOSL2

(GEO: GSM1004810/CistromeDB: 40088) in the promoter region of AIM2 in Th17 cells (Ciofani M et al. 2012). Analyses were performed using the Cistrome Project platform – Cistrome Data Browser tool available at: http://cistrome.org/db/#/.

Cytokine quantification by ELISA

The presence of IL-17 in in the culture supernatant was analyzed by ELISA. Quantification was performed in supernatants using specific mouse IL-17A elisa Kit (R&D cat. DY421), according to the manufacturer's specifications.

QUANTIFICATION AND STATISTICAL ANALYSIS

The analyses of the results were expressed as mean ± standard deviation (SD) and the following statistical tests were performed: one-way ANOVA test followed by Tukey's post-test, or Student's t-test and normality test Gaussian distribution. Such analyses were carried out with the help of the GraphPad Prism software (GraphPad Software Inc., San Diego CA, USA) and differences that presented p values equal to or less than 0.05 were considered statistically significant.